Heliyon 9 (2023) e14152

Contents lists available at ScienceDirect

Heliyon

journal homepage: www.cell.com/heliyon

Research article

N-acetylcysteine (NAC) attenuates quorum sensing regulated phenotypes in *Pseudomonas aeruginosa* PAO1

Emília Maria França Lima [a], Felipe Alves de Almeida [b], Marcelo Palma Sircili [c], Vanessa Bueris [d], Uelinton Manoel Pinto [a,*]

[a] *Food Research Center, Department of Food and Experimental Nutrition, Faculty of Pharmaceutical Sciences, University of Sao Paulo (USP), São Paulo, SP, Brazil*
[b] *Instituto de Laticínios Cândido Tostes (ILCT), Empresa de Pesquisa Agropecuária de Minas Gerais (EPAMIG), Juiz de Fora, MG, Brazil*
[c] *Genetics Laboratory, Butantan Institute, São Paulo, SP, Brazil*
[d] *Microbiology Department, Institute of Biomedical Science, University of São Paulo (USP), São Paulo, SP, Brazil*

ARTICLE INFO

Keywords:
GFP expression
Molecular docking
Pyocyanin
Rhamnolipids
Synergism
Tobramycin

ABSTRACT

The expression of many virulence genes in bacteria is regulated by quorum sensing (QS), and the inhibition of this mechanism has been intensely investigated. *N*-acetylcysteine (NAC) has good antibacterial activity and is able to interfere with biofilm-related respiratory infections, but little is known whether this compound has an effect on bacterial QS communication. This work aimed to evaluate the potential of NAC as a QS inhibitor (QSI) in *Pseudomonas aeruginosa* PAO1 through *in silico* and *in vitro* analyses, as well as in combination with the antibiotic tobramycin. Initially, a molecular docking analysis was performed between the QS regulatory proteins, LasR and RhlR, of *P. aeruginosa* with NAC, 3-oxo-C12-HSL, C4-HSL, and furanone C30. The NAC sub-inhibitory concentration was determined by growth curves. Then, we performed *in vitro* tests using the QS reporter strains *P. aeruginosa lasB-gfp* and *rhlA-gfp*, as well as the expression of QS-related phenotypes. Finally, the synergistic effect of NAC with the antibiotic tobramycin was calculated by fractional inhibitory concentrations index (FIC_i) and investigated against bacterial growth, pigment production, and biofilm formation. In the molecular docking study, NAC bound to LasR and RhlR proteins in a similar manner to the AHL cognate, suggesting that it may be able to bind to QS receptor proteins *in vivo*. In the biosensor assay, the GFP signal was turned down in the presence of NAC at 1000, 500, 250, and 125 μM for *lasB-gfp* and *rhlA-gfp* ($p < 0.05$), suggesting a QS inhibitory effect. Pyocyanin and rhamnolipids decreased ($p < 0.05$) up to 34 and 37%, respectively, in the presence of NAC at 125 μM. Swarming and swimming motilities were inhibited ($p < 0.05$) by NAC at 250 to 10000 μM. Additionally, 2500 and 10000 μM of NAC reduced biofilm formation. NAC-tobramycin combination showed synergistic effect with FIC_i of 0.8, and the best combination was 2500–1.07 μM, inhibiting biofilm formation up to 60%, besides reducing pyocyanin and pyoverdine production. Confocal microscopy images revealed a stronger, dense, and compact biofilm of *P. aeruginosa* PAO1 control, while the biofilm treated with NAC-tobramycin became thinner and more dispersed. Overall, NAC at low concentrations showed promising anti-QS properties against *P. aeruginosa* PAO1, adding to its already known effect as an antibacterial and antibiofilm agent.

* Corresponding author.
E-mail address: uelintonpinto@usp.br (U.M. Pinto).

https://doi.org/10.1016/j.heliyon.2023.e14152
Received 26 July 2022; Received in revised form 22 February 2023; Accepted 22 February 2023
Available online 28 February 2023

1. Introduction

Bacteria have sophisticated communication systems that enable them to send and receive chemical messages to and from other bacteria [1]. This mechanism is known as quorum sensing (QS), which is based on the production, secretion, and response to extracellular signaling molecules called autoinducers (AIs), whose concentration correlate with the populations' cell density [1–3]. QS is stimulated through the recognition of a threshold concentration of AIs, which allows communication between cells, leading to the expression of specific target genes [4,5]. Therefore, this communication enables bacteria to monitor the environment and act as a group, which facilitates population-dependent adaptive behavior, such as bioluminescence, surface motility, biofilm formation, production of toxins, sporulation, conjugative DNA transfer, among others [6–9].

The AIs are chemically diverse molecules and conventionally separated into three major groups. First, *N*-acyl-homoserine lactone (AHL, or AI-1) is a well-known QS system, used by Proteobacteria. Second, a group of molecules derived from 4,5-dihydroxy-2,3-pentanedione (DPD), commonly referred to as AI-2, is found in both Gram-positive and Gram-negative bacteria, and is thought to be a type of interspecies communication mechanism [10,11]. Third, the oligopeptides or auto-inducing peptides (AIPs) are usually secreted by ABC-type carrier proteins and used as signaling molecules by Gram-positive bacteria [3,12]. Additionally, there are several other types of molecules that can also be used as signal molecules among bacteria [3].

Pseudomonas aeruginosa is an opportunistic human pathogen, especially dangerous to cystic fibrosis patients and burn infections [13]. This bacterium expresses many virulence genes through QS regulation, and has become the main model in bacterial anti-virulence strategy studies [14]. The complexity of QS systems in this microorganism is one of the main factors responsible for its selective adaptation and environmental versatility [15].

The QS network of *P. aeruginosa* consists of four interconnected systems, namely *las, rhl, pqs*, and *iqs*, organized in a hierarchical manner. Two synthase/receptor pairs LasI/LasR and RhlI/RhlR, are central to the QS network. LasI resides at the top of the hierarchy, synthesizing the AHL called *N*-3-oxo-dodecanoyl-L-homoserine lactone (3-oxo-C12-HSL), which binds to LasR and directs the expression of various genes. Likewise, RhlI produces *N*-butyryl-L-homoserine lactone (C4-HSL) that binds to its RhlR cognate transcription regulator, activating a suit of other genes [5,16,17].

The *P. aeruginosa* pathogenicity depends on the ability of this bacterium to produce many virulence factors, such as rhamnolipids and pyocyanin, that are under the direct regulation of the QS system by RhlR-RhlI [14,18]. Rhamnolipids are glycolipids that have strong surfactant abilities and play a key role in microbial motility and biofilm development on host surfaces under stressful conditions [15,19,20]. Pyocyanin is a blue pigment and redox-active molecule belonging to the class of phenazines, which is crucial for *P. aeruginosa* virulence, as it is toxic to host cells [21,22].

Since the expression of many virulence factors in bacteria is regulated by QS, there is an increased interest in finding QS inhibitors (QSI). Besides, the emergence of multi-drug resistant bacteria is very worrisome and the use of antibiotics are not always effective in eradicating them and their biofilm [23]. Thus, new non-antibiotic therapies are urgently needed to treat infections and stop the spread of resistant bacteria [24]. Anti-virulence approaches have been widely studied as they can interrupt a pathogen's virulence by inhibiting the production or activity of virulence factors without interfering in bacterial growth and presenting a lower selective pressure against resistance [5,25]. This is one of the reasons to study antimicrobial agents at low concentrations or even to repurpose non-antibiotic drugs as it has been demonstrated with aspirin [26] and ibuprofen [20], both inhibiting QS-regulated phenotypes in *P. aeruginosa*.

N-acetylcysteine (NAC), the *N*-acetyl derivative of the natural amino acid L-cysteine, is a safe and inexpensive medication commercially accessible since the 1960s. It has been used directly or in combination with other medications for treatment of various diseases like chronic bronchitis, asthma and as a mucolytic agent. Besides, NAC acts directly as a scavenger of free radicals, being considered a powerful antioxidant, as demonstrated by several *in vitro* and *in vivo* studies conducted in animals and humans [27,28]. *In vitro* studies have indicated that NAC has good antibacterial properties against Gram-positive and Gram-negative bacteria, and is able to interfere with biofilms-related respiratory infections and for eradicating mature biofilms in the environment [23,29]. Nonetheless, there are no studies demonstrating whether NAC has an effect on bacterial QS communication.

Thus, this work aimed to evaluate the potential of NAC as a QSI in *P. aeruginosa* PAO1 through *in silico* analyses by molecular docking and *in vitro* analyses of QS-regulated phenotypes. In addition, we also evaluated the combined effect of NAC and the antibiotic tobramycin on growth and biofilm formation.

2. Material and methods

2.1. In silico analyses – Molecular modeling and molecular docking of LasR and RhlR proteins of P. aeruginosa PAO1

The molecular docking was performed with LasR and RhlR QS transcriptional regulators of *P. aeruginosa* PAO1.

The crystallized three-dimensional (3D) structure of LasR protein of *P. aeruginosa* PAO1 with different ligands were obtained in the RCSB Protein Data Bank (https://www.rcsb.org/; PDB ID: 2UV0, 6D6A, 6D6L, 6D6O, and 6D6P) [30,31].

The 3D structure of the RhlR protein was not found in any of the databases. Thus, the RhlR protein structure was predicted computationally by molecular modeling. The primary amino acid sequence of RhlR protein was retrieved from UniProtKB database (https://www.uniprot.org/; accession number: P54292). This sequence was used to model the 3D structure using the SWISS-MODEL server (https://swissmodel.expasy.org/interactive) [32] where the templates used were the crystallized 3D structures of the *Escherichia coli* O157:H7 SdiA protein with different ligands (PDB ID: 4Y15 and 4Y17). The quality analysis of the predicted models was

performed using GMQE (Global Model Quality Estimate), QMEAN Z-score, and QMEANDisCo scores on the SWISS-MODEL server [33,34]. The 3D structures were validated by using the Ramachandran plot analysis [35], Verify3D [36], and ERRAT [37] on the SAVES server (https://saves.mbi.ucla.edu).

The molecular docking was performed between LasR and RhlR proteins and their respective AHL cognates, namely 3-oxo-C12-HSL (*N*-(3-oxododecanoyl)-L-homoserine lactone; OdDHL; PubChem CID: 32469421) and C4-HSL (*N*-butyrylhomoserine lactone; BHL; PubChem CID: 443433); besides furanone C30 ((Z-)-4-bromo-5-(bromomethylene)-2(5H)-furanone; PubChem CID: 10131246) and NAC (*N*-acetylcysteine; PubChem CID: 12035). The "Dock Ligands" tool of the CLC Drug Discovery Workbench 4.0 software (https://www.qiagenbioinformatics.com/) was used, with 1,000 interactions for each compound and the conformation of the compounds was changed during the docking via rotation around flexible bonds. The five best docking scores of each compound were selected, allowing the inspection of the binding sites of LasR and RhlR proteins, according to Almeida et al. [38,39].

2.2. Bacterial strains and preparation of compounds

P. aeruginosa PAO1 was used as a wild-type strain. The reporter strains *P. aeruginosa lasB-gfp* and *P. aeruginosa rhlA-gfp* were used for testing NAC as a potential QSI [40]. Both cultures were grown in Luria Bertani (LB) broth at 37 °C.

The compound NAC (Sigma-Aldrich, China) was prepared to obtain stock solutions at 0.1 and 1 M. Furanone C30 (Sigma-Aldrich, Brazil) was prepared to obtain a stock solution at 0.1 M. Antibiotic tobramycin (Sigma-Aldrich, USA) was prepared to obtain a stock solution at 1 mg/mL (2139 μM). All compounds were dissolved in sterile distilled water and stored at −20 °C.

2.3. Antibacterial activity – Minimal inhibitory concentration (MIC)

The minimal inhibitory concentration (MIC) of NAC was determined using the broth microdilution method in a 96-well microplate [41,42]. NAC was applied in serial dilutions ranging from 800 to 25000 μM in LB broth and subsequently, bacterial solution was inoculated (1×10^6 CFU/mL), totaling 100 μL in each well. Optical density at 595 nm (OD 595 nm) was determined every 2 h, during a total time of 24 h in a spectrophotometer (Multiskan FC, Thermo Fisher Scientific). The MIC value was the lowest concentration of NAC in which there was no bacterial growth, as observed on the growth curves. All QS assays were performed at sub-inhibitory concentrations (sub-MICs) to ensure that the compound did not interfere in bacterial growth, as recommended by Defoirdt et al. [43].

2.4. Anti-QS activity

2.4.1. Biosensor assay

The evaluation of NAC as a potential QSI was performed by measuring the expression of green fluorescent protein (GFP) in monitor strains, according to Bjarnsholt et al. (2010). BT-medium (composed of B media (1 mM $MgCl_2$, 0.1 mM $CaCl_2$, and 0.01 mM $FeCl_3$) with 10% A10 (20 g/L $(NH4)_2SO_4$, 60 g/L Na_2HPO_4, 30 g/L KH_2PO_4, and 30 g/L NaCl), 0.025% thiamine, 0.5% glucose, and 0.5% casamino acid; detailed in Bjarnsholt et al. [40]) and NAC were added to each well of microplate to obtain final concentrations ranging from 125 to 1000 μM. Overnight cultures of *P. aeruginosa lasB-gfp* or *P. aeruginosa rhlA-gfp* (1×10^6 CFU/mL) were added, reaching 100 μL in each well. The bacterial growth (OD 450 nm) and GFP expression (excitation/emission wavelength 485/535 nm, respectively) were measured on a multi-mode microplate reader (Synergy H1, Biotek) at 34 °C, every 15 min for 15 h [40]. GFP expression was measured in relative fluorescence units, normalized by dividing the GFP value to the corresponding OD 450 nm value measured at that time point (RFU = GFP/OD 450 nm). The fluorescence peak of the control, *i.e.*, the maximum GFP value, was compared with the peaks of NAC or furanone C30 treatments.

2.4.2. Pyocyanin assay

For pyocyanin assay, *P. aeruginosa* PAO1 was grown in King-A broth (20 g/L peptone, 12 g/L glycerol, 10 g/L K_2SO_4, 1.4 g/L $MgCl_2$) supplemented with 125, 250, and 500 μM of NAC at 37 °C and 250 rpm for 24 h. Supernatants were collected by centrifuging cultures at 10,000 *g* for 10 min (Sigma Laborzentrifugen, Germany), pyocyanin was extracted with chloroform followed by 0.2 N of hydrochloric acid (HCl) and quantified spectrophotometrically at 520 nm [18,44,45]. Results were expressed as percentages (%) of pyocyanin production, comparing absorbance measurements for treatments with NAC and the untreated control, which was considered 100%.

2.4.3. Rhamnolipids assay

For rhamnolipids assay, *P. aeruginosa* PAO1 was grown in LB broth supplemented with 125, 250, and 500 μM of NAC at 37 °C for 24 h. The supernatant was collected by centrifuging cultures at 10,000 *g* for 10 min and acidified with 1 N of HCl to pH 2. Then, 100 μL were transferred to a 96-well microplate and absorbance was measured at 570 nm [45,46]. Results were expressed as percentages (%) of rhamnolipids production, comparing absorbance measurements for treatments with NAC and the untreated control, which was considered 100%.

2.4.4. Swarming and swimming motilities

For the swarming assay, 2 μL of an overnight culture of *P. aeruginosa* PAO1 was inoculated at the center of the swarming agar medium (LB broth with 0.5% (w/v) casamino acids, 0.8% (w/v) glucose, and 0.5% (w/v) agar) with different concentrations of NAC ranging from 0 to 10000 μM [47,48]. For the swimming assay, 2 μL of an overnight culture of *P. aeruginosa* PAO1 was inoculated at the

center of semi-solid LB agar 0.3% (w/v) with different concentrations of NAC ranging from 0 to 10000 μM [42,49]. The swarming and swimming plates were then incubated by 24 h at 37 °C and the motilities diameters were measured and compared with untreated control plates.

2.5. Drug synergy experiments and fractional inhibitory concentration (FIC)

The interaction of NAC with antibiotic tobramycin was investigated by the checkerboard method using 96-well microplates with slight modifications [50,51]. Tobramycin was applied horizontally ranging from 0.53 to 4.28 μM (0.25 to 2 μg/mL) and NAC was applied vertically ranging from 625 to 10000 μM to obtain mixtures of these compounds plus LB broth. Subsequently, bacterial solution at 1×10^6 CFU/mL was inoculated, totaling 200 μL in each well. The microplate was incubated at 37 °C for 24 h. The growth based on visible turbidity and pigments production, such as pyocyanin and pyoverdine, were used for interpreting the results.

The MIC of tobramycin was determined by the broth microdilution method in a 96-well microplate, ranging from 0.25 to 20 μg/mL (0.53 to 42 μM) as described in item 2.3.

The fractional inhibitory concentrations (FIC) and FIC index (FIC_i) were calculated from the following formulas:

$$FIC_i = FIC_{NAC} + FIC_{Tobramycin}$$

Where,

$$FIC_{NAC} = \frac{MIC_{NAC\ in\ combination}}{MIC_{NAC\ alone}};\ FIC_{Tobramycin} = \frac{MIC_{Tobramycin\ in\ combination}}{MIC_{Tobramycin\ alone}}$$

FIC_i values were interpreted as follows: $FIC_i \leq 0.5$ as synergistic; $0.5 < FIC_i \leq 1.0$ as synergistic to additive; $1.0 < FIC_i \leq 4.0$ as indifferent; and $FIC_i > 4.0$ as antagonistic [51,52].

2.6. Effect of NAC-tobramycin combination on P. aeruginosa PAO1 biofilm formation

Biofilm studies were carried out in 96-well microplates in LB broth containing combinations of NAC (0 to 10000 μM) and tobramycin (0 to 4.28 μM), according to Quecán et al. [53]. After incubation at 37 °C for 24 h, the planktonic cells were removed, the adherent biofilm was washed with saline solution 0.85% (w/v) and fixed with methanol (99%) for 15 min, following removal of the solvent. Then, 200 μL of crystal violet solution 0.3% (w/v) were added to each well for 5 min, following removal with sterile water. Finally, the crystal violet bound to the biofilm was extracted with glacial acetic acid 33% (v/v) and the OD 595 nm was measured using the spectrophotometer. Percentage (%) inhibition of biofilm formation was calculated in comparison with control. The synergism was calculated in a SynergyFinder software 3.0 [54].

Confocal laser scanning microscopy (CLSM) was performed with the best combination of NAC-tobramycin, according to Packiavathy et al. [49] with modifications. In a 24-well plate containing a glass coverslip, a total volume of 1000 μL of LB broth, NAC, tobramycin, and bacterial solution at 1×10^6 CFU/mL were added to each well. After 24 h at 37 °C, the supernatants were discarded and the wells were rinsed four times with phosphate-buffered saline (PBS) 1X. Then, 200 μL of 4% *p*-formaldehyde solution in PBS was added to each well and kept for 30 min at room temperature to fix the biofilm on the glass coverslips. Supernatants were discarded and the glass coverslips were rinsed five times with PBS. The glass coverslips were then soaked in 0.2% bovine serum albumin (BSA) solution in PBS for 30 min, in order to block nonspecific staining. After washing three more times with PBS, glass coverslips were fixed on glass slides with Mowiol (Calbiochem) added with 4′,6-diamidino-2-phenylindole (DAPI) dye at a final concentration of 1:1000. Finally, glass coverslips were visualized in the CLSM at 630× magnification (Confocal Leica TCS SP 8, microscope Leica DMi 8, Software Leica LAS X).

2.7. Statistical analysis

The *in vitro* assays of anti-QS activity were performed in three replicates and evaluated by analysis of variance (ANOVA) following Dunnett's test ($p < 0.05$) in Sisvar software version 5.7 [55].

3. Results and discussion

3.1. NAC binds in silico to LasR and RhlR proteins of P. aeruginosa PAO1

Molecular modeling was used to predict the 3D structure of RhlR protein of *P. aeruginosa* PAO1. This process is considered to be the most accurate of the computational structure prediction methods, and has many applications in drug discovery [56].

In the present work, the verification and validation results of the 3D generated structures RhlR named 4Y15-PAO1 and 4Y17-PAO1 revealed that they are reliable (Figs. S1 and S2). The Ramachandran plot analysis showed that more than 96% of the residues of both structures were in favored regions. In addition, both structures had more than 91% of the amino acid residues with scores greater than or equal to 0.2 in the Verify3D, indicating a compatibility between an atomic model (3D) with its own amino acid sequence (1D). Finally, both structures showed a threshold higher than the cut off of 91% in ERRAT overall quality factor (Figs. S1 and S2). Similar results for RhlR protein obtained by homology modeling are reported [57–59].

Molecular docking was performed between different structures of LasR and RhlR proteins of *P. aeruginosa* PAO1 with four compounds: 3-oxo-C12-HSL (Fig. 1A), an AHL synthesized by LasI, which binds to LasR [60]; C4-HSL (Fig. 2A), an AHL synthesized by RhlI, which binds to RhlR [14,61]; NAC (Figs. 1B and 2B), the compound in study, and furanone C30 (Figs. 1C and 2C), a known QSI [62]. This analysis is important to identify a possible QS inhibition, and a possible mechanism, by interference in LuxR-type transcriptional regulators, *i.e.*, LasR and RhlR proteins. The binding affinities and binding amino acid residues are shown in Table 1, Figs. 1 and 2.

The molecular docking assay generates a score which mimics the potential energy change when the protein and the compound interact. The score is based on hydrogen bonds, metal ions and steric interactions, in which lower scores (more negative) correspond to higher binding affinities [39], as it can be observed in Table 1.

The different results obtained for each compound can be explained by the conformational changes of LasR and RhlR proteins when complexed with different compounds, as well as by the structural differences of these compounds. Nonetheless, all compounds were well buried in the active binding pocket of both proteins (Figs. 1G–I and 2G-I), remaining completely inside the pocket (Figs. 1J-L and 2J-L).

For the LasR protein, 3-oxo-C12-HSL showed the highest binding affinities for all analyzed structures (Table 1). Although NAC did not show binding scores as high as those of this AHL, the values were close to those obtained for furanone C30. Furthermore, NAC binding sites were similar to those of 3-oxo-C12-HSL, such as Y56, W60, Y64, D73, T75, and S129 (Table 1, Fig. 1D and E).

Similar results were observed for RhlR protein (Table 1). The C4-HSL also shows the best score, while NAC and furanone C30 presented similar scores. In addition, the binding sites of NAC and C4-HSL were exactly the same for 4Y17 structure, such as Y64, W68, and D81 (Fig. 2D and E). The lack of hydrogen bond in furanone C30 indicates the importance of steric interaction in molecular docking, since the steric interaction is the result of the combination of non-polar interactions, non-polar-polar contacts, and the repulsive contacts (Fig. 2F).

These results indicates that NAC and cognate AHLs potentially compete for binding to the same amino acid residues in both proteins and suggest that NAC may be able to bind to LasR and RhlR proteins equally or better than a known QSI molecule, in this case, furanone C30.

Halogenated furanones produced by the marine red algae *Delisea pulchra* are a well-known group of anti-QS compounds [62]. Furanone C30 is effective at reducing QS-regulated phenotypes and consequently has been used as positive control for QS inhibition in

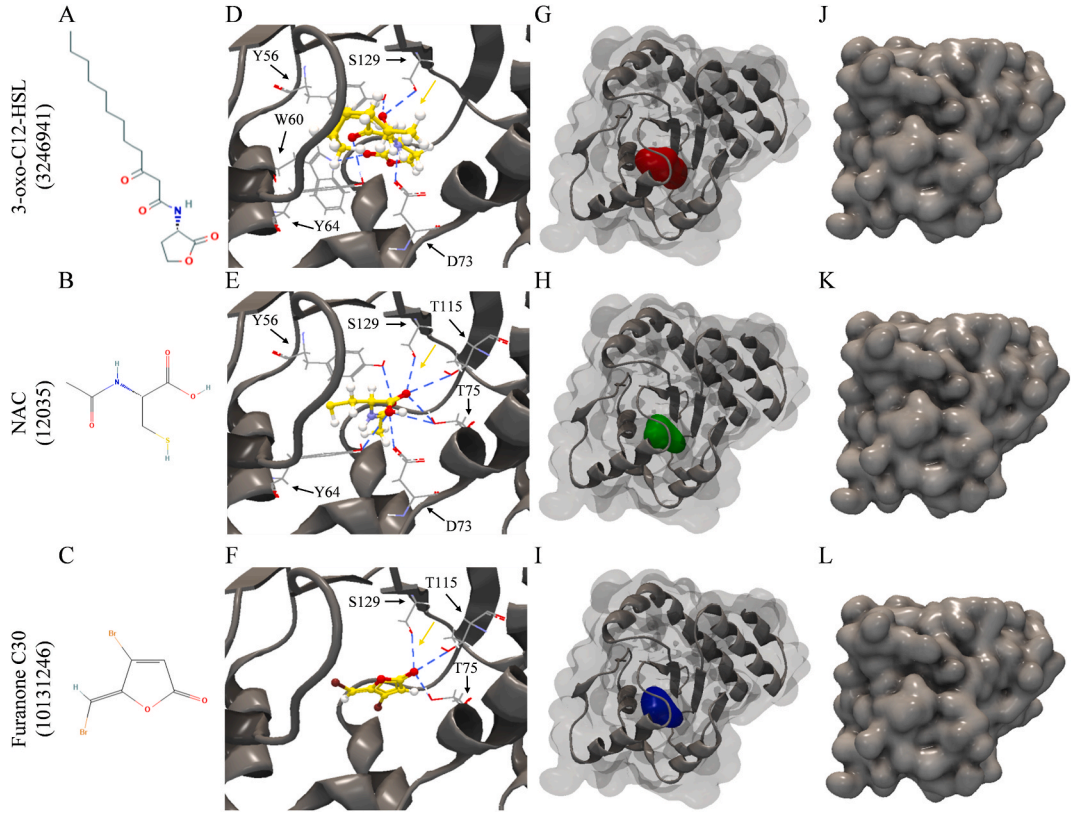

Fig. 1. Molecular docking of 2UV0 structure of LasR protein with 3-oxo-C12-HSL (A), NAC (B), and furanone C30 (C). Backbone representation with hydrogen bond between the amino acid residues and compounds (D to F), surface and backbone representation (G to I) and surface representation showing the compound completely buried in the active binding pocket (J to L). Backbone representation of LasR protein in gray; black arrow indicates the binding site; blue dashed line indicates hydrogen bond. (For interpretation of the references to color in this figure legend, the reader is referred to the Web version of this article.)

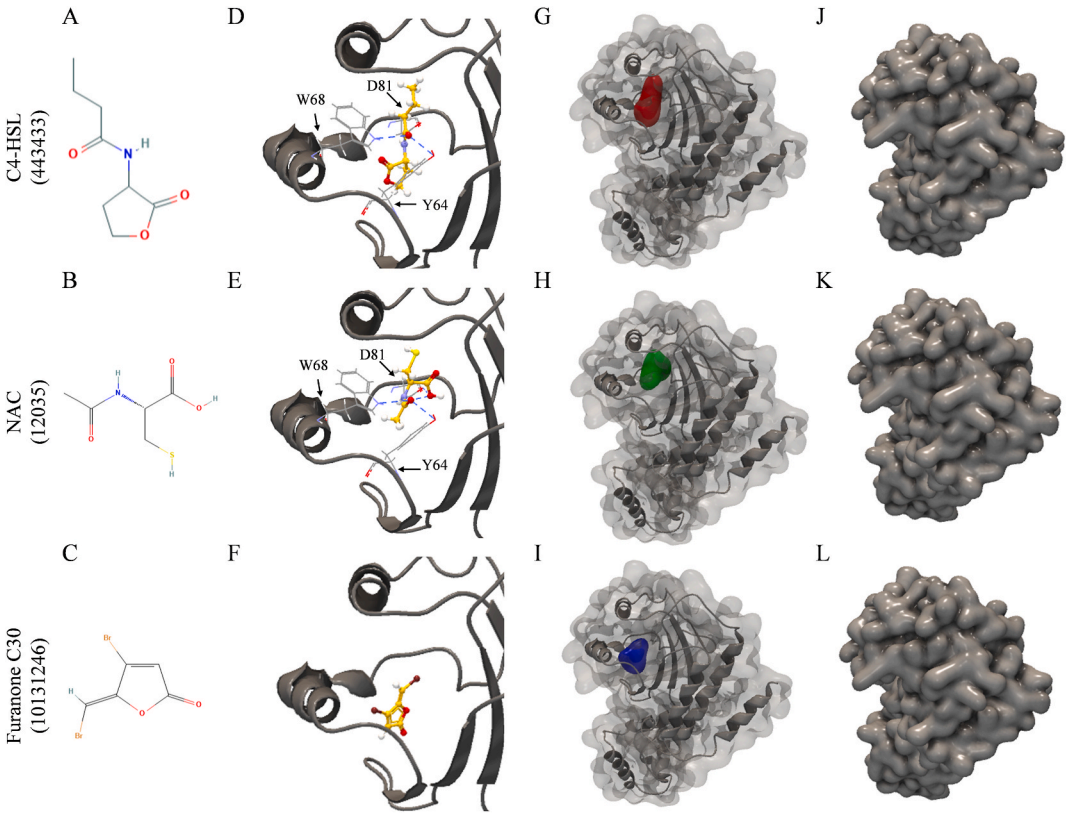

Fig. 2. Molecular docking of 4Y17 structure of RhlR protein with C4-HSL (A), NAC (B), and furanone C30 (C). Backbone representation with hydrogen bond between the amino acid residues and compounds (D to F), surface and backbone representation (G to I) and surface representation showing the compound completely buried in the active binding pocket (J to L). Backbone representation of RhlR protein in gray; black arrow indicates the binding site; blue dashed line indicates hydrogen bond. (For interpretation of the references to color in this figure legend, the reader is referred to the Web version of this article.)

Table 1
Results of molecular docking of different structures of LasR and RhlR proteins of *P. aeruginosa* PAO1 with 3-oxo-C12-HSL, C4-HSL, NAC, and furanone C30.

Protein - structure	Molecule	Binding residue	Hydrogen bond score	Steric interaction score	Score total	Rank
LasR - 2UV0	3-oxo-C12-HSL	Y56, W60, Y64, D73, S129	−10.12	−77.05	−81.77	1
	NAC	Y56, Y64, D73, T75, T115, S129	−13.11	−28.49	−39.91	2
	Furanone C30	T75, T115, S129	−6.00	−31.95	−37.95	3
LasR - 6D6A	3-oxo-C12-HSL	Y56, Y64, T75, S129	−8.00	−72.68	−76.01	1
	NAC	Y56, D73, T75, T115, S129	−15.10	−26.76	−39.89	2
	Furanone C30	T75, T115, S129	−6.00	−32.08	−38.08	3
LasR - 6D6L	3-oxo-C12-HSL	Y56	−3.37	−78.54	−75.73	1
	NAC	W60, D73, T75, T115, S129	−13.99	−29.64	−41.96	3
	Furanone C30	T75, T115, S129	−7.34	−38.45	−45.78	2
LasR - 6D6O	3-oxo-C12-HSL	Y56, W60, S129	−6.90	−74.04	−76.36	1
	NAC	Y56, W60, T75, T115, S129	−11.68	−33.49	−43.03	3
	Furanone C30	T75, T115, S129	−7.71	−38.71	−46.42	2
LasR - 6D6P	3-oxo-C12-HSL	Y56, D73	−5.08	−78.74	−77.73	1
	NAC	W60, D73, T75, T115	−9.19	−34.57	−42.22	3
	Furanone C30	T75, T115, S129	−6.90	−38.05	−44.95	2
RhlR - 4Y15-PAO1	C4-HSL	Y64	−4.00	−41.17	−43.90	1
	NAC	D81, Y64, Y72, S135	−8.00	−25.84	−32.36	3
	Furanone C30	No binding	0.00	−33.90	−33.90	2
RhlR - 4Y17-PAO1	C4-HSL	Y64, W68, D81	−6.79	−39.91	−45.54	1
	NAC	Y64, W68, D81	−8.93	−29.07	−36.65	2
	Furanone C30	No binding	0.00	−34.81	−34.81	3

many experiments, including inhibition of violacein production, biofilm formation and swarming motility [53,63]. Concerning the QS inhibition mechanism, Paczkowski et al. [48] showed that furanones function non-competitively by destabilizing LasR protein and promoting its degradation. Unfortunately, furanones exhibit toxicity to human cells and their use is not suitable in human hosts as therapeutic agents [48,64,65].

3.2. Sub-MICs of NAC inhibit QS systems of *P. aeruginosa*

The growth curves of *P. aeruginosa* PAO1 showed that 25000 μM of NAC completely inhibited the bacterial growth (Fig. 3A). Concentrations lower than 12500 μM, *i.e.*, 6200, 3100, 1500, and 800 μM did not influence the growth of this bacterium at the evaluated condition. Hence, these concentrations were used in the QS inhibition tests to ensure that NAC did not interfere in bacterial growth in the QS related bioassays.

The use of reporter strains is an important asset to evaluate whether a compound potentially inhibits QS. For this assay, we used *P. aeruginosa* PAO1 harboring either a *lasB-gfp* or a *rhlA-gfp* fusion, which produce a modified and unstable version of GFP, as a QS reporter. So, expression of *gfp* gives rise to a burst of fluorescence when *lasB* or *rhlA* is induced, which are QS-regulated genes. This system is very sensitive, and the GFP signal is turned down in the presence of a QSI [40].

In the present study, the fluorescence peak of untreated control was compared with other peaks. The GFP signal was reduced ($p < 0.05$) in the presence of 50 μM of furanone C30 by 76% for *lasB-gfp* and 60% for *rhlA-gfp*. NAC also significantly inhibited ($p < 0.05$) both QS systems. For *lasB* expression, the best inhibitory concentrations were 500 μM (88%) and 1000 μM (85%). For *rhlA* expression, the best inhibitory concentrations were 250 μM (17%) and 125 μM (16%), compared to the fluorescence peak of the untreated control

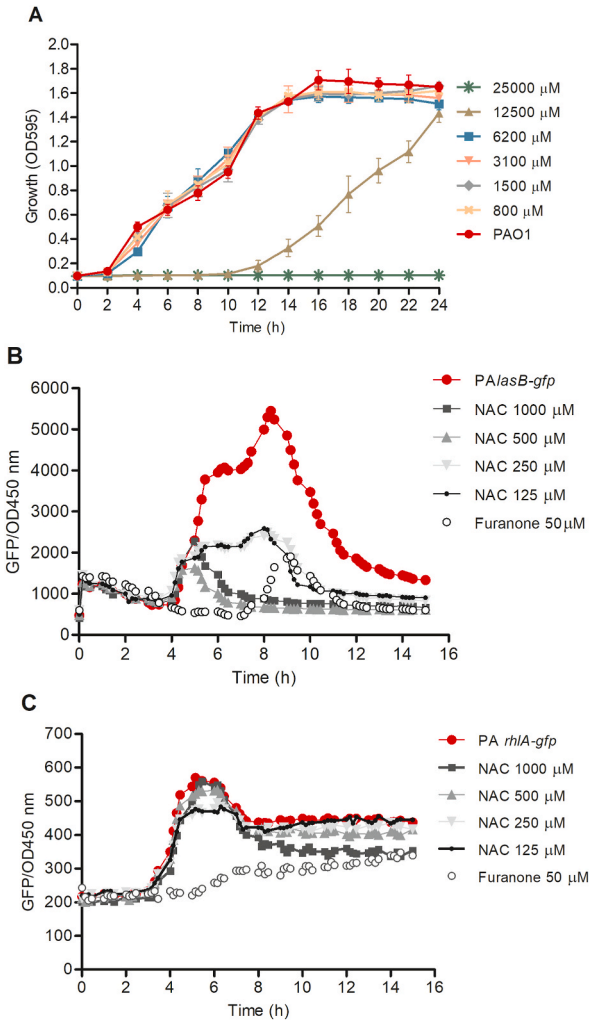

Fig. 3. Growth curves of *P. aeruginosa* PAO1 with concentrations ranging from 800 to 25000 μM of NAC in LB broth at 37 °C for 24 h (A). Dose-response curves of *P. aeruginosa lasB-gfp* (B) and *rhlA-gfp* (C) monitor strains treated with concentrations ranging from 125 to 1000 μM of NAC and 50 μM of furanone C30. Data shown as mean values ± standard error of three replicates and data shown as mean values of three replicates.

(Fig. 3B and C). Thus, we expected that NAC would have a greater effect in inhibiting phenotypes regulated by the *las* system in this assay. However, since the QS network is robust and interconnected in *P. aeruginosa*, an interference with LasI/LasR, which is at the top of the hierarchical network, will likely influence the expression of the other systems and their respective virulence factors. This is the case for pyocyanin and rhamnolipids, which are regulated by RhlI/RhlR and will be discussed below.

Many compounds have been identified as QSI by the same biosensor strains. Jakobsen et al. [19] found that ajoene, the major bioactive compound present in garlic extract, is capable of inhibiting the expression of *lasB-gfp* and *rhlA-gfp* fusion in a dose-dependent manner, in concentrations ranging from 6.7 to 854 μM. Gökalsın et al. [66] showed that the carotenoid zeaxanthin at 12 μM inhibited *las* and *rhl* QS systems by 68 and 66%, respectively, when compared to the untreated control group. Beenker et al. [67] tested the effect of gregatins, a group of related fungal secondary metabolites, on GFP expression of *lasB-gfp, rhlA-gfp* and *pqsA-gfp* QS reporter strains, in concentrations ranging from 15.6 to 2000 μM. They observed that gregatins had the least effect or no effect on the *rhlA-gfp* reporter, similar to the result found in the present study with NAC.

3.3. Sub-MICs of NAC inhibited pyocyanin, rhamnolipids, and motility

Pyocyanin and rhamnolipids are virulence factors that play an important role in biofilm development, in the establishment of infection and colonization of the host by *P. aeruginosa* [45]. Both are under control of QS; therefore, their inhibition is a good indicator of QS inhibition. Here, pyocyanin production decreased 19, 22, and 34% in the presence of NAC at 500, 250, and 125 μM, respectively ($p < 0.05$) (Fig. 4A and Table S1). In these same concentrations, the rhamnolipids production was decreased by 28, 33, and 37%, respectively ($p < 0.05$) (Fig. 4B and Table S1). Similar results were observed by Dai et al. [20] for ibuprofen at 100 μg/mL, which reduced the production of pyocyanin up to 24% and rhamnolipids up to 34% by *P. aeruginosa*. Natural compounds, such as 6-gingerol at 100 μM [63], coumarins at 2000 μM [68], and naringenin at 4000 μM [69] were also reported as inhibitors of pyocyanin and rhamnolipids production by *P. aeruginosa*.

In the present study, we observed that the inhibition of these phenotypes was not concentration-dependent, since all three tested concentrations inhibited ($p < 0.05$) both virulence factors statistically equally (Fig. 4A and B). Other studies have also reported similar

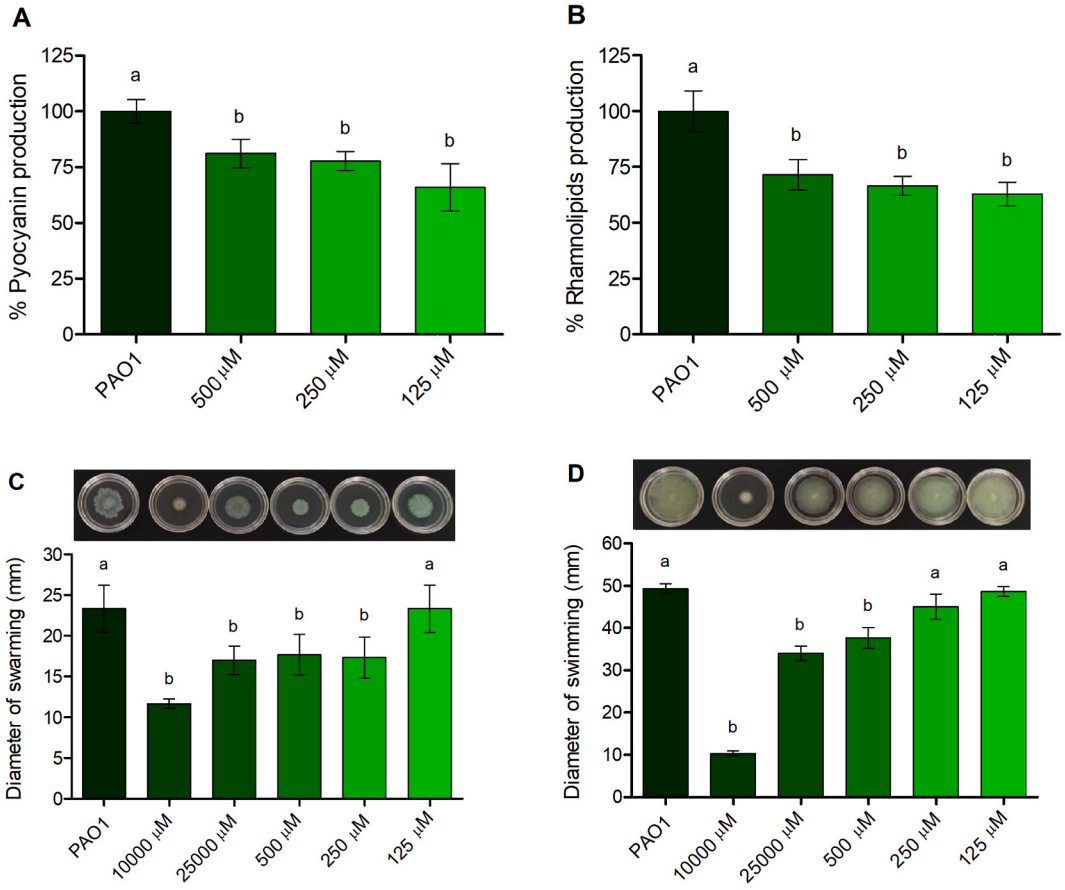

Fig. 4. Effect of NAC at different concentrations on the production of pyocyanin (A) and rhamnolipids (B), swarming (C) and swimming motilities (D) when compared to the control (*P. aeruginosa* PAO1 without NAC). Data shown as mean values ± standard error of three replicates. Means followed by different letters differ ($p < 0.05$) by Dunnett's test and by the same letters do not differ ($p > 0.05$).

results. For instance, Beenker et al. [67] observed that increasing concentrations of gregatins from 15 to 2000 μM exhibited different behaviors in biofilm formation, pyocyanin and rhamnolipids production, showing nonlinear inhibitions, with the highest concentration not always having the best inhibition. Likewise, Dai et al. [20] evaluated the levels of 3-oxo-C12-HSL and C4-HSL in *P. aeruginosa* with ibuprofen at different concentrations and time points and they did not observe a concentration-dependent inhibitory effect of this compound.

Since rhamnolipids are involved in swarming motility due to surfactant properties, we hypothesized that NAC would inhibit this type of motility. Swarming motility is an organized microbial movement on surfaces, dependent on extensive flagellation, cell–cell contact and QS, which contributes to biofilm formation and infection [70]. The swimming motility allows bacterial movement on semisolid surfaces, which is important in absorption of nutrients and biofilm formation [49,71]. Both motilities are strongly associated with pathogenesis in *P. aeruginosa* since they enable bacteria to colonize environments, attach to different surfaces and to form biofilms [70,72]. So, we examined the anti-QS potential of NAC against both types of motilities, in concentrations up to 10000 μM, which were the same tested in the biofilm assay. As observed in Fig. 4, the highest tested concentrations of NAC (500, 2500, and 10000 μM) statistically inhibited swarming (Fig. 4C and Table S2) and swimming (Fig. 4D and Table S2) motilities. Furthermore, the concentration of 10000 μM of NAC inhibited swimming motility about 80%. On the contrary, no inhibition was observed for the lowest concentration of NAC (125 μM). Other studies have also reported the inhibition of swarming and/or swimming motilities of *P. aeruginosa* with potential QSIs, like curcumin at 50, 75, and 100 μg/mL [49], furanones at 7.5 mM [72], methyl gallate ranging from 16 to 256 μg/mL [47], and 5-hydroxymethylfurfural at 1.25 μL/mL [73].

3.4. NAC-tobramycin combination has effect on bacterial growth, pigment production, and biofilm formation

Antimicrobial resistance is a serious concern in clinical practice, and an emergent strategy in combating resistant bacteria is the coadministration of antibiotics with other compounds [42,50,74]. The synergistic activity of two drugs is achieved if they have different modes of action and such action can bring about a higher killing effect on the bacteria [50]. Here, the idea is that NAC would

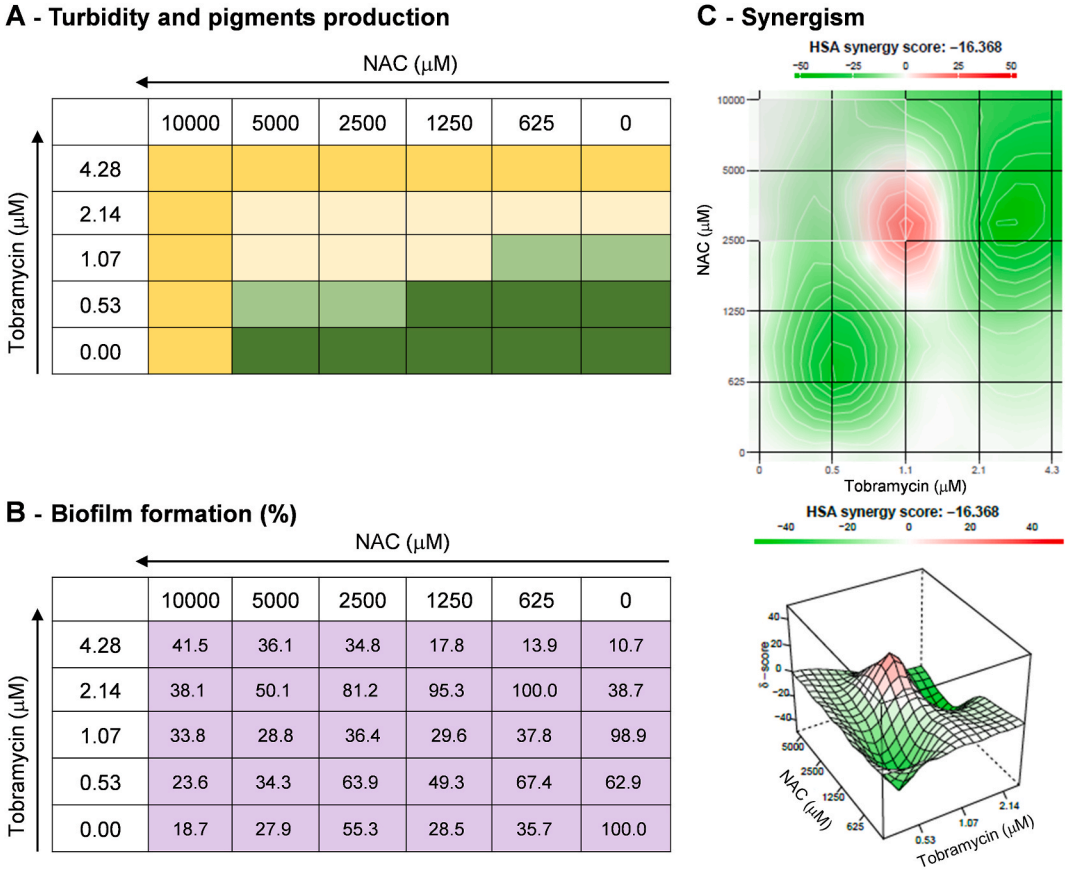

Fig. 5. Checkerboard assay showing effect of NAC-tobramycin combinations against *P. aeruginosa* PAO1. Yellow color represents growth inhibition (additive/MIC); cream color indicates synergistic effect with lower growth inhibition and no production of pigments; green color shows no effect, no reduction in growth based on the visible turbidity and on pigments production (A). Result of biofilm formation by crystal violet assay (B). Synergy maps in 2D and 3D plots of biofilm formation; red color shows synergism while green color shows no reduction of biofilm formation (no-synergy) (C). (For interpretation of the references to color in this figure legend, the reader is referred to the Web version of this article.)

work as a QSI, acting in the inhibition of cellular communication, and, consequently, on the attenuation of virulence factors, while tobramycin works through a cell killing effect.

Tobramycin belongs to aminoglycoside class of antibiotics and is commonly used to treat *P. aeruginosa* infections as well as infections from other susceptible organisms including *Serratia, Proteus, Acinetobacter,* and *Klebsiella.* Tobramycin is one of the most commonly monitored aminoglycosides in clinical laboratories, together with amikacin and gentamicin [75]. Besides, it is the main antibiotic recommended to treat chronic bacterial infections [76,77].

NAC-tobramycin combination against *P. aeruginosa* PAO1 showed a synergistic effect with FIC_i of 0.8, considering MIC of NAC alone (25000 μM), MIC of NAC combined (10000 μM), MIC of tobramycin alone (5.35 μM), and MIC of tobramycin combined (2.14 μM). The data on the effectiveness of NAC-tobramycin combinations against this bacterium are represented in a checkerboard, observed visually (Fig. 5A). The observation of low turbidity and lack of pigment production (pyocyanin and pyoverdine), characteristics of *P. aeruginosa*, indicated the inhibitory effect of drug combinations. The highest concentration of NAC (10000 μM) and the highest concentration of tobramycin (4.28 μM), alone or in combination, were effective in partially inhibiting growth and the production of pigments. The lowest concentrations that reduced pigment production were 5000, 2500, and 1250 μM of NAC combined with 1.07 μM tobramycin (Fig. 5A).

For biofilm assay, the first step was to treat the formed biofilm with crystal violet, and the result is shown in Fig. 5B and Table S3. It is possible to observe that the highest concentrations of NAC and tobramycin alone reduced the biofilm formation of *P. aeruginosa* PAO1 by 81% and 89%, respectively (Fig. 5B). These data were analyzed in the synergism assay, and the combination of 2500–1.07 μM (NAC-tobramycin) was the most synergistic combination for inhibiting biofilm formation, as observed in Fig. 5C. In the synergism assay, the summary synergy scores can be interpreted as the average excess response due to drug interactions. For example, a synergy score of 10 corresponds to 10% of response beyond expectation [54,78]. In the present study, the global score was negative (−16.368), indicating that the interaction is likely to be antagonistic. The score of most synergistic area (MSA, which represents the most synergistic 3-by-3 dose-window in a dose-response matrix, Fig. 5C) is near zero (−2.66), indicating an additive interaction. However, the score in the red point (2500–1.07 μM of NAC-tobramycin) is 26.24, indicating a synergistic interaction at this combination. In this scenario, biofilm formation was inhibited by 63.5% (Fig. 5B). This is an interesting result because these drug concentrations are lower than MIC, and the use of low concentrations may prevent the development of resistance.

In this scenario, we evaluate the formed biofilm in different conditions by using confocal laser scanning microscopy (Fig. 6). CLSM images for *P. aeruginosa* PAO1 (Fig. 6A) revealed a stronger, dense and compact biofilm. We observed that treatment with NAC altered the biofilm architecture. Fig. 6B and C showed a biofilm thinner and more spaced, besides it is possible to visualize the background of

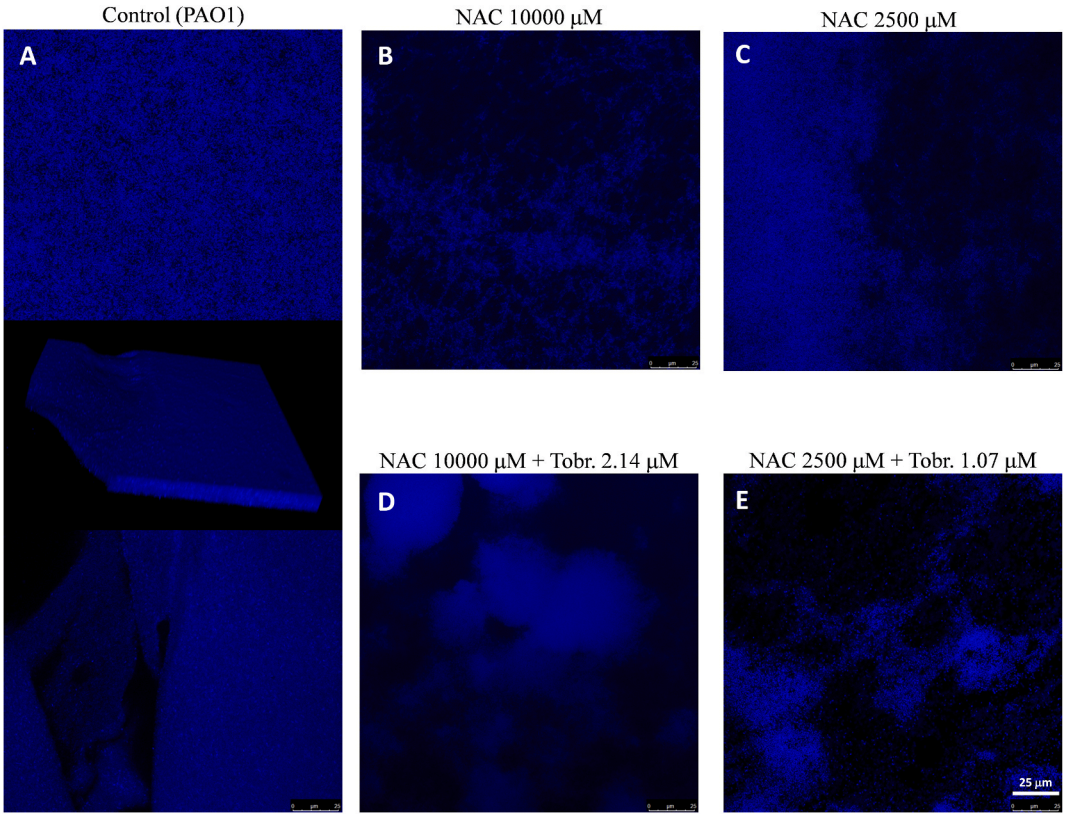

Fig. 6. Biofilms formed on glass coverslips by *P. aeruginosa* PAO1 (A) in the presence of NAC at 10000 μM (B) and 2500 μM (C), as well as in the presence of NAC in combination with tobramycin (Tobr.) at 10000 μM + 2.14 μM (D) and 2500 μM + 1.07 μM (E).

the slide. These changes were greater in the combinations of NAC-tobramycin (Fig. 6D and E), since CLSM images showed an even less dense biofilm. The most synergistic combination, 2500–1.07 μM of NAC-tobramycin (Fig. 6E) also showed the dispersed and thinner biofilm with spaced adhered cells, proving the efficiency of the drug combination. NAC can increase the sensitivity of *P. aeruginosa* to tobramycin and is a potential agent to be co-administered with antibiotics.

Quorum sensing regulates the expression of many genes associated with biofilm formation, and biofilms are associated with reduced sensitivity to antibiotics [79]. Thus, QS interference can be explored as an alternative to reduce bacterial virulence and increase the efficacy of antibiotic treatment. The combination of QSIs with antibiotics was demonstrated by Mion et al. [79], combining lactonases with fluoroquinolones and efficiently decreasing the amount of antibiotics required to fight *P. aeruginosa* clinical isolates. The flavonoid quercetin exhibited synergism between tobramycin and amikacin, providing better anti-biofilm activity against *P. aeruginosa* strains compared to their MIC dose [50]. Combinations of gallic acid-ampicillin and hamamelitannin-erythromycin inhibited the growth, biofilm viability, and motilities of *Escherichia coli* better than individual antibiotics, being promising candidates for eradicating pathogenic *E. coli* in humans and animals, according to Hossain et al. [51].

Finally, it is important consider that the virulence factors, motility, and biofilm formation are controlled by many pathways and molecules, in addition to quorum sensing. Thus, it is important to identify the exact target and mechanism of inhibitory compounds to ensure the influence on QS pathways [80]. For instance, more robust analysis could be performed, such as molecular and genetic techniques, gene expression assays of target QS genes, molecular dynamic analysis, and *in vivo* assays with animal models. Besides, it is necessary to treat bacteria with a specific concentration range, since low concentrations may not show an anti-QS effect, whereas high concentrations may be toxic or influence bacterial growth [67]. Here, in some tests, we used concentrations well below the MIC, and higher concentrations may present even better results for inhibiting the tested phenotypes.

4. Conclusion

To our knowledge, this is the first study to show NAC as a potential QSI against *P. aeruginosa* PAO1. The *in silico* analyses suggest a possible inhibitory mechanism, since NAC interacts with LasR and RhlR proteins similarly to cognate AHLs and, sometimes, even better than the QSI furanone C30. Assays with biosensor strains and QS-related phenotypes demonstrated the *in vitro* inhibitory potential, besides swarming and swimming motilities were strongly inhibited at the same concentration of NAC that inhibited biofilm formation The combination of NAC-tobramycin seems to be an interesting way to reduce the drug dose and inhibit biofilm formation by *P. aeruginosa* PAO1, as visualized by confocal microscopy. We suggest further studies to evaluate the expression of QS target genes of *P. aeruginosa* PAO1 in the presence of NAC in different concentrations and in combination with tobramycin to elucidate the mechanism of action, as well as to perform *in vivo* assays with animal models and also test other strains of *P. aeruginosa*.

Author contribution statement

Emília Maria França Lima: Conceived and designed the experiments; Performed the experiments; Analyzed and interpreted the data; Wrote the paper.

Felipe Alves de Almeida: Analyzed and interpreted the data; Wrote the paper.

Marcelo Palma Sircili: Contributed reagents, materials, analysis tools or data.

Vanessa Bueris: Contributed reagents, materials, analysis tools or data.

Uelinton Manoel Pinto: Conceived and designed the experiments; Contributed reagents, materials, analysis tools or data; Wrote the paper.

Funding statement

Prof. Uelinton Manoel Pinto was supported by Fundação de Amparo à Pesquisa do Estado de São Paulo (FAPESP) [2013/07914-8], and Conselho Nacional de Desenvolvimento Científico e Tecnológico (CNPq) [422242/2018-7]. Emília Maria França Lima received scholarship from Coordenação de Aperfeiçoamento de Pessoal de Nível Superior (CAPES).

Data availability statement

Data included in article/supp. material/referenced in article.

Declaration of interest's statement

The authors declare no competing interests.

Acknowledgment

We would like to thank the Cellular Biology Laboratory of Butantan Institute and the staff Alexsander Seixas de Souza for the services provided by the Confocal Leica TCS SP 8 – Project 175 FINEP – IBUINFRA 01.12.0175.00 Dr. Carlos Jared. We also thank CLC Bio of the QIAGEN Company for the license of the CLC Drug Discovery Workbench 4.0 software.

Appendix A. Supplementary data

Supplementary data to this article can be found online at https://doi.org/10.1016/j.heliyon.2023.e14152.

References

[1] B.L. Bassler, R. Losick, Bacterially speaking, Cell 125 (2006) 237–246, https://doi.org/10.1016/j.cell.2006.04.001.
[2] W.C. Fuqua, S.C. Winans, E.P. Greenberg, Quorum sensing in bacteria: the LuxR-LuxI family of cell density-responsive transcriptional regulators, J. Bacteriol. 176 (1994) 269–275.
[3] E.M.F. Lima, B.X. Valencia, L. Quecán, R. da Cunha, B. D, G. de, M. Franco, U.M. Pinto, Cell-cell communication in lactic acid bacteria - potential mechanisms, in: M.A.C. de Albuquerque, A. de M. de LeBlanc, J.G. LeBlanc, R. Bedani (Eds.), Lact. Acid Bact. A Funct. Approach, 2020, pp. 1–14, https://doi.org/10.1007/978-3-319-60021-5_1.
[4] L.A. Hawver, S.A. Jung, W.L. Ng, Specificity and complexity in bacterial quorum-sensing systems, FEMS Microbiol. Rev. 40 (2016) 738–752, https://doi.org/10.1093/femsre/fuw014.
[5] K.A. Simanek, I.R. Taylor, E.K. Richael, E. Lasek-nesselquist, The PqsE-RhlR interaction regulates RhlR DNA binding to control virulence factor production in Pseudomonas aeruginosa, Microbiol. Spectr. 10 (2022) e02108–e02121.
[6] S. Azimi, A.D. Klementiev, M. Whiteley, S.P. Diggle, Bacterial quorum sensing during infection, Annu. Rev. Microbiol. 74 (2020) 201–219, https://doi.org/10.1146/annurev-micro-032020-093845.
[7] L. Wu, Y. Luo, Bacterial quorum-sensing systems and their role in intestinal bacteria-host crosstalk, Front. Microbiol. 12 (2021) 1–11, https://doi.org/10.3389/fmicb.2021.611413.
[8] J. van Gestel, T. Bareia, B. Tenennbaum, A. Dal Co, P. Guler, N. Aframian, S. Puyesky, I. Grinberg, G.G. D'Souza, Z. Erez, M. Ackermann, A. Eldar, Short-range quorum sensing controls horizontal gene transfer at micron scale in bacterial communities, Nat. Commun. 12 (2021) 1–11, https://doi.org/10.1038/s41467-021-22649-4.
[9] M.A. Welsh, H.E. Blackwell, Chemical genetics reveals environment-specific roles for quorum sensing circuits in Pseudomonas aeruginosa, Cell Chem. Biol. 23 (2016) 361–369, https://doi.org/10.1016/j.chembiol.2016.01.006.
[10] X. Chen, S. Schauder, N. Potier, A. Van Dorsselaer, I. Pelczer, B.L. Bassler, F.M. Hughson, Structural identification of a bacterial quorum-sensing signal containing boron, Nature 415 (2002) 545–549, https://doi.org/10.1038/415545a.
[11] C.S. Pereira, J.A. Thompson, K.B. Xavier, AI-2-mediated signalling in bacteria, FEMS Microbiol. Rev. 37 (2013) 156–181, https://doi.org/10.1111/j.1574-6976.2012.00345.x.
[12] V. Monnet, V. Juillard, R. Gardan, Peptide conversations in Gram-positive bacteria, Crit. Rev. Microbiol. 42 (2014) 339–351, https://doi.org/10.3109/1040841X.2014.948804.
[13] Z. Pang, R. Raudonis, B.R. Glick, T. Lin, Z. Cheng, Antibiotic resistance in Pseudomonas aeruginosa: mechanisms and alternative therapeutic strategies, Biotechnol. Adv. 37 (2019) 177–192, https://doi.org/10.1016/j.biotechadv.2018.11.013.
[14] J. Lee, L. Zhang, The hierarchy quorum sensing network in Pseudomonas aeruginosa, Protein Cell 6 (2014) 26–41, https://doi.org/10.1007/s13238-014-0100-x.
[15] A.A. Jack, S. Khan, L.C. Powell, M.F. Pritchard, K. Beck, H. Sadh, L. Sutton, A. Cavaliere, H. Florance, P.D. Rye, D.W. Thomas, E. Hill, Alginate oligosaccharide-induced modification of the lasI-lasR and rhlI-rhlR quorum-sensing systems in Pseudomonas aeruginosa, Antimicrob. Agents Chemother. 62 (2018) 1–14, https://doi.org/10.1128/AAC.02318-17.
[16] T. Defoirdt, Quorum-sensing systems as targets for antivirulence therapy, Trends Microbiol. 26 (2018) 313–328, https://doi.org/10.1016/j.tim.2017.10.005.
[17] M.C.D. Vanetti, D.G. Carneiro, F.A. de Almeida, E.L.G. Vargas, E.M.F. Lima, U.M. Pinto, Autoinducer-1 quorum sensing communication mechanism in gram-negative bacteria, in: V.R. Rai, J.A. Bai (Eds.), Trends Quor. Sens. Quor. Quenching - New Perspect. Appl., 2020, pp. 9–30.
[18] S.A.K.S. Ahmed, M. Rudden, T.J. Smyth, J.S.G. Dooley, R. Marchant, I.M. Banat, Natural quorum sensing inhibitors effectively downregulate gene expression of Pseudomonas aeruginosa virulence factors, Appl. Microbiol. Biotechnol. (2019) 3521–3535, https://doi.org/10.1007/s00253-019-09618-0.
[19] T.H. Jakobsen, M. Van Gennip, R.K. Phipps, M.S. Shanmugham, L.D. Christensen, M. Alhede, M.E. Skindersoe, T.B. Rasmussen, K. Friedrich, F. Uthe, P. Ø. Jensen, C. Moser, K.F. Nielsen, L. Eberl, T.O. Larsen, D. Tanner, N. Høiby, T. Bjarnsholt, M. Givskov, Ajoene, a sulfur-rich molecule from garlic, inhibits genes controlled by quorum sensing, Antimicrob. Agents Chemother. 56 (2012) 2314–2325, https://doi.org/10.1128/AAC.05919-11.
[20] L. Dai, T. qi Wu, Y. song Xiong, H. bing Ni, Y. Ding, W. chen Zhang, S. peng Chu, S. qing Ju, J. Yu, Ibuprofen-mediated potential inhibition of biofilm development and quorum sensing in Pseudomonas aeruginosa, Life Sci. 237 (2019), 116947, https://doi.org/10.1016/j.lfs.2019.116947.
[21] L.A. Meirelles, D.K. Newman, Both toxic and beneficial effects of pyocyanin contribute to the lifecycle of Pseudomonas aeruginosa, Mol. Microbiol. 110 (2018) 995–1010, https://doi.org/10.1111/mmi.14132.
[22] S. Sarabhai, P. Sharma, N. Capalash, Ellagic acid derivatives from Terminalia chebula retz. Downregulate the expression of quorum sensing genes to attenuate Pseudomonas aeruginosa PAO1 virulence, PLoS One 8 (2013) 1–11, https://doi.org/10.1371/journal.pone.0053441.
[23] F. Blasi, C. Page, G.M. Rossolini, L. Pallecchi, M.G. Matera, P. Rogliani, M. Cazzola, The effect of N-acetylcysteine on biofilms: implications for the treatment of respiratory tract infections, Respir. Med. 117 (2016) 190–197, https://doi.org/10.1016/j.rmed.2016.06.015.
[24] P. Venkatesan, Collaborate to stop antimicrobial resistance - for the sake of the planet, Lan. Microb. 2 (2021) e497, https://doi.org/10.1016/S2666-5247(21)00248-2.
[25] T. Defoirdt, Specific antivirulence activity, a new concept for reliable screening of virulence inhibitors, Trends Biotechnol. 34 (2016) 527–529, https://doi.org/10.1016/j.tibtech.2016.01.009.
[26] S.A. El-mowafy, K.H. Abd, E. Galil, S.M. El-messery, M.I. Shaaban, Microbial Pathogenesis Aspirin is an ef fi cient inhibitor of quorum sensing , virulence and toxins in Pseudomonas aeruginosa, Microb. Pathog. 74 (2014) 25–32, https://doi.org/10.1016/j.micpath.2014.07.008.
[27] G. Aldini, A. Altomare, G. Baron, G. Vistoli, M. Carini, L. Borsani, F. Sergio, N-Acetylcysteine as an antioxidant and disulphide breaking agent: the reasons why, Free Radic. Res. 52 (2018) 751–762, https://doi.org/10.1080/10715762.2018.1468564.
[28] V. Mokhtari, P. Afsharian, M. Shahhoseini, S.M. Kalantar, A. Moini, A review on various uses of N-acetyl cysteine, Cell J 19 (2017) 11–17.
[29] M. Nowacka, A. Rygała, D. Kręgiel, A. Kowalewska, Poly(silsesquioxanes) and poly(siloxanes) grafted with N-acetylcysteine for eradicating mature bacterial biofilms in water environment, Colloids Surf., B 172 (2018) 627–634, https://doi.org/10.1016/j.colsurfb.2018.09.017.
[30] M.C. O'Reilly, S.-H. Dong, F.M. Rossi, K.M. Karlen, R.S. Kumar, S.K. Nair, H.E. Blackwell, Structural and biochemical studies of non-native agonists of the LasR quorum-sensing receptor reveal an L3 Loop "Out" conformation for LasR, Cell Chem. Biol. 25 (2018) 1128–1139.e3, https://doi.org/10.1016/j.chembiol.2018.06.007.
[31] M.J. Bottomley, E. Muraglia, R. Bazzo, A. Carfi, Molecular insights into quorum sensing in the human pathogen Pseudomonas aeruginosa from the structure of the virulence regulator LasR bound to its autoinducer, J. Biol. Chem. 282 (2007) 13592–13600, https://doi.org/10.1074/jbc.M700556200.
[32] A. Waterhouse, M. Bertoni, S. Bienert, G. Studer, G. Tauriello, R. Gumienny, F.T. Heer, T.A.P. De Beer, C. Rempfer, L. Bordoli, R. Lepore, T. Schwede, SWISS-MODEL: homology modelling of protein structures and complexes, Nucleic Acids Res. 46 (2018) 296–303, https://doi.org/10.1093/nar/gky427.
[33] P. Benkert, M. Biasini, T. Schwede, Toward the estimation of the absolute quality of individual protein structure models, Bioinformatics 27 (2011) 343–350, https://doi.org/10.1093/bioinformatics/btq662.
[34] G. Studer, C. Rempfer, A.M. Waterhouse, R. Gumienny, J. Haas, T. Schwede, QMEANDisCo-distance constraints applied on model quality estimation, Bioinformatics 36 (2020) 1765–1771, https://doi.org/10.1093/bioinformatics/btz828.
[35] S.C. Lovell, I.W. Davis, W.B.A. Iii, P.I.W. De Bakker, J.M. Word, M.G. Prisant, J.S. Richardson, D.C. Richardson, Structure validation by Cα geometry: φ, ψ and Cβ deviation, Proteins Struct. Funct. Genet. 50 (2003) 437–450.

[36] R. Lüthy, J.U. Bowie, D. Eisenberg, Assessment of proten models with three-dimensional profiles, Nature 356 (1992) 83–85.
[37] C. Colovos, T. Yeates, Verification of protein structures : patterns of nonbonded atomic interactions, Protein Sci. 2 (1993) 1511–1519.
[38] F.A. Almeida, U.M. Pinto, M.C.D. Vanetti, Novel insights from molecular docking of SdiA from Salmonella Enteritidis and Escherichia coli with quorum sensing and quorum quenching molecules, Microb. Pathog. 99 (2016) 178–190, https://doi.org/10.1016/j.micpath.2016.08.024.
[39] F.A. Almeida, E.L.G. Vargas, D.G. Carneiro, U.M. Pinto, M.C.D. Vanetti, Virtual screening of plant compounds and nonsteroidal anti-inflammatory drugs for inhibition of quorum sensing and biofilm formation in Salmonella, Microb. Pathog. 121 (2018) 369–388, https://doi.org/10.1016/j.micpath.2018.05.014.
[40] T. Bjarnsholt, M. Van Gennip, T.H. Jakobsen, L.D. Christensen, P. Jensen, M. Givskov, In vitro screens for quorum sensing inhibitors and in vivo confirmation of their effect, Nat. Protoc. 5 (2010) 282–293, https://doi.org/10.1038/nprot.2009.205.
[41] I. Wiegand, K. Hilpert, R.E.W. Hancock, Agar and broth dilution methods to determine the minimal inhibitory concentration (MIC) of antimicrobial substances, Nat. Protoc. 3 (2008) 163–175, https://doi.org/10.1038/nprot.2007.521.
[42] C.A. Santos, E.M.F. Lima, B.D.G. de, M. Franco, U.M. Pinto, Exploring phenolic compounds as quorum sensing inhibitors in foodborne bacteria, Front. Microbiol. 12 (2021), https://doi.org/10.3389/fmicb.2021.735931.
[43] T. Defoirdt, G. Brackman, T. Coenye, Quorum sensing inhibitors: how strong is the evidence? Trends Microbiol. 21 (2013) 619–624, https://doi.org/10.1016/j.tim.2013.09.006.
[44] D.W. Essar, L. Eberly, A. Hadero, I.P. Crawford, Identification and characterization of genes for a second anthranilate synthase in Pseudomonas aeruginosa: interchangeability of the two anthranilate synthase and evolutionary implications, J. Bacteriol. 172 (1990) 884–900.
[45] V.K. Singh, A. Mishra, B. Jha, 3-Benzyl-Hexahydro-Pyrrolo[1,2-a]Pyrazine-1,4-Dione extracted from exiguobacterium indicum showed anti-biofilm activity against Pseudomonas aeruginosa by attenuating quorum sensing, Front. Microbiol. 10 (2019), https://doi.org/10.3389/fmicb.2019.01269.
[46] C.D. McClure, N.L. Schiller, Effects of Pseudomonas aeruginosa rhamnolipids on human monocyte-derived macrophages, J. Leukoc. Biol. 51 (1992) 97–102, https://doi.org/10.1002/jlb.51.2.97.
[47] M.A. Hossain, S.J. Lee, N.H. Park, A.F. Mechesso, B.T. Birhanu, J. Kang, M.A. Reza, J.W. Suh, S.C. Park, Impact of phenolic compounds in the acyl homoserine lactone-mediated quorum sensing regulatory pathways, Sci. Rep. 7 (2017) 1–16, https://doi.org/10.1038/s41598-017-10997-5.
[48] J.E. Paczkowski, S. Mukherjee, A.R. McCready, J.P. Cong, C.J. Aquino, H. Kim, B.R. Henke, C.D. Smith, B.L. Bassler, Flavonoids suppress Pseudomonas aeruginosa virulence through allosteric inhibition of quorum-sensing Receptors, J. Biol. Chem. 292 (2017) 4064–4076, https://doi.org/10.1074/jbc.M116.770552.
[49] I.A.S.V. Packiavathy, S. Priya, S.K. Pandian, A.V. Ravi, Inhibition of biofilm development of uropathogens by curcumin - an anti-quorum sensing agent from Curcuma longa, Food Chem. 148 (2014) 453–460, https://doi.org/10.1016/j.foodchem.2012.08.002.
[50] C. Vipin, K. Saptami, F. Fida, M. Mujeeburahiman, S.S. Rao, Athmika, A.B. Arun, P.D. Rekha, Potential synergistic activity of quercetin with antibiotics against multidrug-resistant clinical strains of Pseudomonas aeruginosa, PLoS One 15 (2020) 1–15, https://doi.org/10.1371/journal.pone.0241304.
[51] M.A. Hossain, H.C. Park, S.W. Park, S.C. Park, M.G. Seo, M. Her, J. Kang, Synergism of the combination of traditional antibiotics and novel phenolic compounds against escherichia coli, Pathogens 9 (2020) 1–23, https://doi.org/10.3390/pathogens9100811.
[52] I. Shalit, Y. Shadkchan, Z. Samra, N. Osherov, In vitro synergy of caspofungin and itraconazole against Aspergillus spp.: MIC versus minimal effective concentration end points, Antimicrob. Agents Chemother. 47 (2003) 1416–1418, https://doi.org/10.1128/AAC.47.4.1416-1418.2003.
[53] B.X. V Quecan, J.T.C. Santos, M.L.C. Rivera, N.M.A. Hassimotto, F.A. Almeida, U.M. Pinto, Effect of quercetin rich onion extracts on bacterial quorum sensing, Front. Microbiol. 10 (2019), https://doi.org/10.3389/fmicb.2019.00867.
[54] A. Ianevski, A.K. Giri, T. Aittokallio, SynergyFinder 3.0 : an interactive analysis and consensus interpretation of multi-drug synergies across multiple samples, Nucleic Acids Res. (2022) 1–5.
[55] D.F. Ferreira, Sisvar: a Guide for its Bootstrap procedures in multiple comparisons, Cienc. E Agrotecnol 38 (2014) 109–112, https://doi.org/10.1590/s1413-70542014000200001.
[56] M.T. Muhammed, E. Aki-Yalcin, Homology modeling in drug discovery: overview, current applications and future perspectives, Chem. Biol. Drug Des. 93 (2018) 12–20, https://doi.org/10.1111/cbdd.13388.
[57] A. Shukla, P. Parmar, B. Patel, D. Goswami, M. Saraf, Breaking bad: better call gingerol for improving antibiotic susceptibility of Pseudomonas aeruginosa by inhibiting multiple quorum sensing pathways, Microbiol. Res. 252 (2021), 126863, https://doi.org/10.1016/j.micres.2021.126863.
[58] S. Skariyachan, R. Ravishankar, D. Gopal, A.G. Muddebihalkar, A. Uttarkar, P. Kaveramma, U. Praveen, V. Niranjan, Infection, Genetics and Evolution Response regulator GacA and transcriptional activator RhlR proteins involved in bio fi lm formation of Pseudomonas aeruginosa are prospective targets for natural lead molecules : computational modelling , molecular dockin, Infect. Genet. Evol. 85 (2020), 104448, https://doi.org/10.1016/j.meegid.2020.104448.
[59] E. Önem, H.C. Sarısu, A.G. Özaydın, M.T. Muhammed, A. Ak, Phytochemical profile, antimicrobial, and anti-quorum sensing properties of fruit stalks of Prunus avium L, Lett. Appl. Microbiol. 73 (2021) 426–437, https://doi.org/10.1111/lam.13528.
[60] J.P. Pearson, K.M. Gray, L. Passador, K.D. Tucker, A. Eberhard, B.H. Iglewski, E.P. Greenberg, Structure of the autoinducer required for expression of Pseudomonas aeruginosa virulence genes, Proc. Natl. Acad. Sci. USA 91 (1994) 197–201, https://doi.org/10.1073/pnas.91.1.197.
[61] J.P. Pearson, L. Passador, B.H. Iglewski, E.P. Greenberg, A second N-acylhomoserine lactone signal produced by Pseudomonas aeruginosa, Proc. Natl. Acad. Sci. USA 92 (1995) 1490–1494, https://doi.org/10.1073/pnas.92.5.1490.
[62] S. Kjelleberg, P. Steinberg, M. Givskov, L. Gram, M. Manefield, R. De Nys, Do marine natural products interfere with prokaryotic AHL regulatory systems? Aquat. Microb. Ecol. 13 (1997) 85–93, https://doi.org/10.3354/ame013085.
[63] H.S. Kim, S.H. Lee, Y. Byun, H.D. Park, 6-Gingerol reduces Pseudomonas aeruginosa biofilm formation and virulence via quorum sensing inhibition, Sci. Rep. 5 (2015), https://doi.org/10.1038/srep08656.
[64] A. Lamin, A.H. Kaksonen, I.S. Cole, X.B. Chen, Quorum sensing inhibitors applications: a new prospect for mitigation of microbiologically influenced corrosion, Bioelectrochemistry 145 (2022), 108050, https://doi.org/10.1016/j.bioelechem.2022.108050.
[65] B. LaSarre, M.J. Federle, Exploiting quorum sensing to confuse bacterial pathogens, Microbiol. Mol. Biol. Rev. 77 (2013) 73–111, https://doi.org/10.1128/MMBR.00046-12.
[66] B. Gökalsın, B. Aksoydan, B. Erman, N.C. Sesal, Reducing virulence and biofilm of Pseudomonas aeruginosa by potential quorum sensing inhibitor carotenoid: zeaxanthin, Microb. Ecol. 74 (2017) 466–473, https://doi.org/10.1007/s00248-017-0949-3.
[67] W.A.G. Beenker, J. Hoeksma, J. Den Hertog, Gregatins, a group of related fungal secondary metabolites, inhibit aspects of quorum sensing in gram-negative bacteria, Front. Microbiol. 13 (2022) 1–15, https://doi.org/10.3389/fmicb.2022.934235.
[68] Y. Zhang, A. Sass, H. Van Acker, J. Wille, B. Verhasselt, F. Van Nieuwerburgh, V. Kaever, A. Crabbé, T. Coenye, Coumarin reduces virulence and biofilm formation in Pseudomonas aeruginosa by affecting quorum sensing, type III secretion and C-di-GMP levels, Front. Microbiol. 9 (2018) 1–10, https://doi.org/10.3389/fmicb.2018.01952.
[69] S. Hernando-Amado, M. Alcalde-Rico, T. Gil-Gil, J.R. Valverde, J.L. Martínez, Naringenin inhibition of the Pseudomonas aeruginosa quorum sensing response is based on its time-dependent competition with N-(3-oxo-dodecanoyl)-L-homoserine lactone for LasR binding, Front. Mol. Biosci. 7 (2020) 1–11, https://doi.org/10.3389/fmolb.2020.00025.
[70] S. Rütschlin, T. Böttcher, Inhibitors of bacterial swarming behavior, Chem. Eur J. 26 (2020) 964–979, https://doi.org/10.1002/chem.201901961.
[71] T. Ding, T. Li, J. Li, Discovery of quorum sensing inhibitors of Pseudomonas fluorescens P07 by using a receptor-based pharmacophore model and virtual screening, LWT–Food Sci. Technol. 109 (2019) 171–178, https://doi.org/10.1016/j.lwt.2019.04.030.
[72] L.M. Otton, M. da S. Campos, K.L. Meneghetti, G. Corção, Influence of twitching and swarming motilities on biofilm formation in Pseudomonas strains, Arch. Microbiol. 199 (2017) 677–682, https://doi.org/10.1007/s00203-017-1344-7.
[73] J. Rajkumari, S. Borkotoky, D. Reddy, S.K. Mohanty, R. Kumavath, A. Murali, K. Suchiang, S. Busi, Anti-quorum sensing and anti-biofilm activity of 5-hydroxymethylfurfural against Pseudomonas aeruginosa PAO1: insights from in vitro, in vivo and in silico studies, Microbiol. Res. 226 (2019) 19–26, https://doi.org/10.1016/j.micres.2019.05.001.

[74] J.W. Zhou, T.T. Chen, X.J. Tan, J.Y. Sheng, A.Q. Jia, Can the quorum sensing inhibitor resveratrol function as an aminoglycoside antibiotic accelerant against Pseudomonas aeruginosa? Int. J. Antimicrob. Agents 52 (2018) 35–41, https://doi.org/10.1016/j.ijantimicag.2018.03.002.
[75] A. Dasgupta, in: G.S. Makowski (Ed.), Advances in Antibiotic Measurement, Adv. Clin. Chem., 2012, pp. 75–104, https://doi.org/10.1016/B978-0-12-394317-0.00013-3.
[76] C. Castellani, A.J.A. Duff, S.C. Bell, H.G.M. Heijerman, A. Munck, F. Ratjen, I. Sermet-gaudelus, K.W. Southern, J. Barben, P.A. Flume, P. Hodková, N. Kashirskaya, M.N. Kirszenbaum, S. Madge, H. Oxley, B. Plant, S. Jane, A.R. Smyth, G. Taccetti, T.O.F. Wagner, S.P. Wolfe, P. Drevinek, ECFS best practice guidelines: the 2018 revision, J. Cyst. Fibros. 17 (2018) 153–178, https://doi.org/10.1016/j.jcf.2018.02.006.
[77] P.J. Mogayzel, E.T. Naureckas, K.A. Robinson, G. Mueller, D. Hadjiliadis, J.B. Hoag, L. Lubsch, L. Hazle, K. Sabadosa, B. Marshall, C. Practice, G. Committee, Occasional essay cystic fibrosis pulmonary guidelines chronic medications for maintenance of lung health, Am. J. Respir. Crit. Care Med. 187 (2013) 680–689, https://doi.org/10.1164/rccm.201207-1160OE.
[78] A. Ianevski, A.K. Giri, T. Aittokallio, SynergyFinder 2.0: visual analytics of multi-drug combination synergies, Nucleic Acids Res. 48 (2020) 488–493, https://doi.org/10.1093/NAR/GKAA216.
[79] S. Mion, B. Rémy, L. Plener, F. Brégeon, E. Chabrière, D. Daudé, A.M. Otero, Quorum quenching lactonase strengthens bacteriophage and antibiotic arsenal against Pseudomonas aeruginosa clinical isolates, Front. Microbiol. 10 (2019) 1–11, https://doi.org/10.3389/fmicb.2019.02049.
[80] D. Deryabin, A. Galadzhieva, D. Kosyan, G. Duskaev, Plant-derived inhibitors of AHL-mediated quorum sensing in bacteria: modes of action, Int. J. Mol. Sci. 20 (2019), https://doi.org/10.3390/ijms20225588.